Studying the release of hGH from gamma-irradiated PLGA microparticles using ATR-FTIR imaging

KELES, Hakan, NAYLOR, Andrew, CLEGG, Francis and SAMMON, Chris

Published version

KELES, Hakan, NAYLOR, Andrew, CLEGG, Francis and SAMMON, Chris (2014). Studying the release of hGH from gamma-irradiated PLGA microparticles using ATR-FTIR imaging. Vibrational Spectroscopy, 71, 76-84.

Vibrational Spectroscopy 71 (2014) 76–84

Contents lists available at ScienceDirect

Vibrational Spectroscopy

journal homepage: www.elsevier.com/locate/vibspec

Studying the release of hGH from gamma-irradiated PLGA microparticles using ATR-FTIR imaging☆

Hakan Keles[a], Andrew Naylor[b], Francis Clegg[a], Chris Sammon[a,*]

[a] Sheffield Hallam University, Materials and Engineering Research Institute, Sheffield S1 1WB, United Kingdom
[b] Critical Pharmaceuticals Limited, BioCity, Pennyfoot Street, Nottingham NG1 1GF, United Kingdom

ARTICLE INFO

Article history:
Received 1 November 2013
Received in revised form 15 January 2014
Accepted 24 January 2014
Available online 2 February 2014

Keywords:
Microparticle
PLGA
Protein
Controlled release
ATR-FTIR imaging
Gamma-irradiation

ABSTRACT

Attenuated total reflection-Fourier transform infrared (ATR-FTIR) imaging has been applied for the first time to monitor the redistribution and release of hGH from a range of PLGA/PLA microparticles during a set of dissolution experiments at 37 °C in D_2O. The effect of gamma-irradiation, a common sterilisation method, on hGH release kinetics from such systems has been demonstrated. Increasing the gamma dose was shown to have a profound influence on the nature of the release mechanism, with higher gamma doses leading to a dramatic increase in the initial burst release followed by a retardation in the sustained release and a lower total level of hGH release over the dissolution experiment. These changes were shown to be the result of a combination of factors; firstly, *via* scanning electron microscopy (SEM), gamma-irradiation was shown to strongly influence the morphology of the PLGA/PLA microparticles; reducing their overall porosity and reducing the available surface area, whilst forcing some of the entrapped hGH to the microparticle surface. Secondly, from FTIR measurements, gamma-irradiation was shown to increase the number of oxygenated components in the Poloxamer 407 excipient, by a process of chain scission, thereby increasing the strength of interaction between the microparticle and the entrapped hGH.

1. Introduction

Peptides and proteins cannot readily be delivered by traditional routes such as by oral, nasal or pulmonary delivery due to their high molecular weight, hydrophilicity and labile nature. Consequently such drugs are normally administered by injection to therapeutically tackle a number of conditions. To treat growth hormone (hGH, a 22 kDa protein) deficiency in children with hypopituitary disorders and in adults, this normally results in the need for daily injections for a period of several years which is particularly challenging for children. Encapsulation of drugs such as proteins in biodegradable polymer matrices, such as PLGA for sustained release, offers a solution to the problem of delivery of drugs effectively to the patient with minimal inconvenience and also controlling drug's release into the body over time, thereby removing the necessity for frequent administration and improving patient compliance and treatment efficacy.

A sustained release formulation of hGH can be achieved by its encapsulation into injectable microparticles of biodegradable and biocompatible polymers such as PLGA or PLA. After injection the encapsulated microparticle slowly releases the hGH *via* a degradation mechanisms of the polymer to lactic or glycolic acid which are rapidly cleared from the body *via* the renal system.

To date solvent-based methods such as emulsification have been most often used to manufacture PLGA based microparticle drug delivery systems. However, the use of solvents can lower the biological activity of any encapsulated protein or peptide through degradation at phase boundaries [1]. One route to overcome these difficulties is to use supercritical carbon dioxide ($scCO_2$) that removes the need for solvents during processing, such as in the PGSS (particles from gas saturated solutions) method for the production of sustained release systems including polymer matrix microparticles [2]. Novel sustained release formulations of hGH prepared by supercritical fluid processing of PLGA/PLA (the CriticalMix™ process) were produced in the form of microparticles for subcutaneous injection [3]. We have taken a formulation that has been evaluated *in vivo* in rats and monkeys, showing up to two weeks more of efficacious hGH release compared to a daily injection of soluble hGH, and investigated its real time release using ATR-FTIR imaging for the first time. This study also evaluates the effect of γ-irradiation on the physical and chemical structure of the

☆ Selected paper presented at 7th International Conference on Advanced Vibrational Spectroscopy, Kobe, Japan, August 25–30, 2013.

* Corresponding author. Tel.: +44 0114 225 3069; fax: +44 0114 225 3501.
E-mail address: C.Sammon@shu.ac.uk (C. Sammon).

0924-2031/$ – see front matter © 2014 Published by Elsevier B.V.
http://dx.doi.org/10.1016/j.vibspec.2014.01.012

microparticles and attempts to draw links between chemical and morphological changes and the *in vivo* release of the entrapped hGH from single microparticles.

Pharmaceutically relevant microparticles for parenteral use must be well characterised in terms of their size range, morphology and function. It is widely understood that the chemistry and morphology of microparticles have a degree of interdependence as the morphology of microspheres can vary depending on their chemical state after preparation. This therefore can strongly affect drug release behaviour from microspheres [4–6].

Often, pharmaceuticals have to be sterilised before use and for polymeric microparticle drug delivery systems, γ-irradiation is a well-established method to achieve this [6,7]. Prior to sterilisation of pharmaceutical products using γ-irradiation, it is essential to determine any effects that this process may have on the materials, as each polymer reacts differently to ionising radiation. Therefore the maximum dose that can be administered to sterilise the product must to be validated.

Fourier transform infrared (FTIR) spectroscopic imaging facilitates spatiotemporal images of individual components of multicomponent systems under dynamic conditions such as dissolution [8]. It has become a popular spectroscopic imaging approach, particularly for pharmaceutical research, as it allows not only monitoring the physical and chemical changes of individual components over time, but also gives quantitative information such as drug release rate and polymer matrix degradation rate from the same experiment [8–10].

Collecting thousands of IR spectra simultaneously using a 2D focal plane array detector in which each pixel acts as an individual detector, a stack of 2D images at a range of mid-IR energies can be generated within a few minutes.

The application of the attenuated total reflectance (ATR) sampling technique in FTIR imaging has been increasingly reported particularly in pharmaceutical research [11,12] as it is advantageous compared to transmission and transflection FTIR mainly in that the shallow (2–10 μm) depth of penetration (*i.e.* the depth at which the electric field amplitude is attenuated to e^{-1} of its initial value at the sample surface) of IR light in to the sample facilitates the visualisation of formulations within aqueous media (as the water bands cannot suppress the signal from the sample as a result of this shallow penetration depth) and species can be probed in their natural state as no sample preparation is necessary [13].

Micro-ATR-FTIR imaging with a Ge internal reflection element (IRE) provides higher spatial resolution when compared to transmission and transflection measurements but with a much smaller field of view [14]. Consequently, ATR-FTIR imaging in macro mode in which the infrared beam from the spectrometer is passed through the IRE and collected at the FPA without the use of a microscope is more convenient compared to micro-ATR as it provides a larger field of view and readily facilitates the use of a temperature controlled environment for studying dynamic systems [15].

FTIR spectroscopy has been used for studying the interactions of carbohydrates with dried proteins [16], assessing the integrity of the hGH encapsulated in PLGA by spray-freeze-drying and water-in-oil-in-water double emulsion methods [17] and assessing the effect of excipients in lysozyme and BSA loaded microspheres prepared by a double-emulsion technique [18]. The lysozyme distribution in microtomed PLGA microspheres prepared by a w-o-w solvent evaporation method has been studied by FTIR imaging in transmission mode and the second derivative protein amide I band images shown a homogenous distribution of protein [19]. The use of real time FTIR imaging for characterisation of a drug delivery system [9] and dissolution of tablets [20,21] has been demonstrated. Although distinct sample-solvent interfaces along one axis of the field of view were monitored and release and redistribution of various active pharmaceutical ingredients (APIs) were investigated in these FTIR imaging studies, there is no literature regarding demonstration of the application of real time FTIR imaging to (i) study the release of proteins or peptides from biodegradable microparticles *in situ* and (ii) the assessment of the effect of γ-irradiation on stability of PLGA microparticles and on the release of the protein from the microparticles, therefore our study aims to address these aspects of vibrational spectroscopy applied to pharmaceutical research. Generally, kinetic processes such as release (including the burst release phenomenon, which is critically important for assessing sustained release from drug delivery devices) and matrix degradation in protein based API loaded biopolymer microparticles are monitored by a combination of various conventional methods including; differential scanning calorimetry (DSC), gel permeation chromatography (GPC), x-ray diffraction and infrared (IR) absorption spectroscopies [6], nuclear magnetic resonance (NMR) and electron paramagnetic resonance (EPR) spectroscopies [5] and UV–vis spectrophotometry [3] on bulk samples (*i.e.* multiple microparticles). This paper demonstrates the possibility of obtaining such important quantitative chemical information by using FTIR spectroscopic imaging alone on a single microparticle which allows the morphological visualisation of the kinetic processes involved, which is not available by bulk methods.

2. Experimental

2.1. Materials

PLGA RG502H (50:50 lactide:glycolide, I.V. 0.16–0.24, Bohringer-Ingleheim) with an inherent viscosity of 0.16–0.24 dl/g, PLA R202H (100:0 lactide:glycolide, I.V. 0.16–0.24, Bohringer-Ingleheim), with an inherent viscosity of 0.16–0.24 dl/g, pharmaceutical grade CO_2 (BOC Special Gasses) were used as received. hGH was kindly donated by Bioker (Sardinia, Italy) and Poloxamer 407 (Lutrol® F127) was obtained from BASF (Ludwigshafen, Germany). D_2O (613398-10G, min. 99.996 atom) and bee's wax (243248-100G) were purchased from Sigma–Aldrich Company Limited, UK. Technovit 7100 embedding resin kit was purchased from Kulzer & Co., Germany.

2.2. Preparation of microparticles using $scCO_2$ processing

The method of PGSS (particles from gas saturated solutions) uses the ability of $scCO_2$ to depress the glass transition and melting temperature of biodegradable polymers at ambient temperatures and moderate pressures. $scCO_2$ acts effectively as a molecular lubricant, thus liquefying polymers at temperatures significantly lower than those typically needed. The near ambient temperatures together with the absence of any aqueous or organic solvents makes the PGSS method particularly suited to the processing of thermally or solvent labile proteins and peptides, with the advantage that they can be encapsulated with 100% efficiency with no protein degradation or loss of activity.

A formulation of hGH loaded PLGA/PLA microparticles were prepared using a CriticalMix™ process by adding 2 g of pre-weighed combination of spray dried hGH (10%, w/w of the formulation), PLGA and PLA in 90:10 ratio respectively (81%, w/w of the formulation) and GRAS excipient, Poloxamer407 (9%, w/w of the formulation), to the PGSS apparatus which was sealed and pressurised with CO_2 to 700 psi (48 bar) and once heated to above 32 °C the pressure was increased to 2030 psi (140 bar). The $scCO_2$ was dissolved into the liquefied mixture which was then stirred at 150 rpm for 1 h, after which time stirring was stopped and the homogenous mixture was depressurised through a nozzle generating free flowing microparticles into a collection chamber [3].

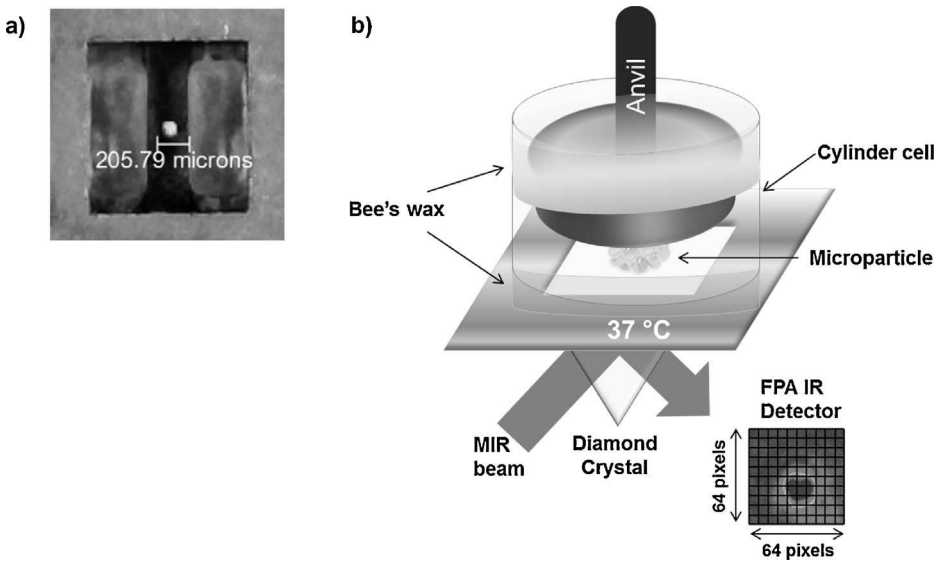

Fig. 1. (a) White light image of a microparticle placed on the ATR crystal prior to starting the experiment. (b) Schematic of the dissolution experiment; the anvil applies sufficient pressure to ensure good contact between the particle and the ATR crystal, whilst making sure D_2O can only access the particles from the sides.

2.3. Sample preparation for micro-ATR-FTIR imaging

hGH loaded PLGA/PLA microparticles were embedded in a hydroxyethyl methacrylate based resin (Technovit 7100) as described by van de Weert et al. [19] and sliced to 4 μm thickness using a Reichert-Jung Ultracut E ambient ultramicrotome with a glass knife.

2.4. Scanning electron microscopy

To obtain topographic contrast of the microspheres before and after irradiation, scanning electron microscopy (SEM) was performed using a FEI NOVA 200 NanoSEM. Images were formed using the secondary electron signal with a spatial resolution of ~2 nm. The sample was sprinkled onto an adhesive carbon tab on an aluminium stub and sputter coated with gold (~20 nm) in an Argon atmosphere.

2.5. γ-Irradiation

Raw polymers and $scSO_2$ produced microparticle formulations were irradiated by using ^{60}Co as irradiation source (Synergy Health PLC, Swindon, UK) at a few kGy/h dose rates ensuring a targeted total dose in accordance with the ISO 11137 standard. The sample temperature was kept at near room temperature during irradiation using thermometric controls. 30 mg of the polymer samples were sealed in a glass container and irradiated at 25 and 100 kGy total dose in air.

2.6. ATR-FTIR spectroscopy

ATR-FTIR spectra were collected on a Thermo Nicolet Nexus instrument as single beam spectra by co-adding 128 scans at a spectral resolution of 4 cm^{-1} and ratioed against the single beam spectrum of the blank ATR crystal at room temperature.

2.7. Micro-ATR-FTIR imaging

Micro-ATR-FTIR images were collected with the setup that consists of an Agilent 680-IR FT-IR spectrometer operating in rapid scan mode attached to an Agilent 620-IR microscope with a Ge ATR crystal fitted on to a 15× Cassegrain objective and a liquid nitrogen cooled mercury cadmium telluride focal plane array detector MCT-FPA (64 × 64 pixels).

Images were collected with a 4 cm^{-1} spectral resolution in the mid-infrared range (3800–950 cm^{-1}) co-adding 64 scans for both background (Ge crystal in air) and samples. The high refractive index (4) of the germanium crystal allowed a spatial resolution of ~4 μm within the ~64 μm × 64 μm field of view for this setup.

2.8. Macro-ATR-FTIR imaging of drug release from individual microparticles

Mid-infrared (3800–950 cm^{-1}) spectroscopic imaging data in Macro-ATR mode were acquired using an Agilent 680-IR FT-IR spectrometer attached to a large sample (LS) external compartment holding a Golden Gate™ Imaging Single Reflection ATR Accessory (Specac Ltd.) which has a Diamond internal reflection element with corrective optics that adjusts the plane of best focus to sit on the crystal surface minimising any distortion. The infrared beam from the spectrometer was projected directly on to a liquid nitrogen cooled MCT-FPA (64 × 64 pixels, 10 μm × 10 μm pixel size) after passing through the ATR sampling accessory. This ATR-FTIR imaging setup was capable of simultaneously collecting 4096 spectra from an image area of 640 μm × 640 μm with an angle of incidence of the infrared beam of 45° and numerical aperture (NA) of 0.32.

A single microparticle was placed on to the centre of the square surface of the ATR crystal with the aid of a 40× binocular microscope. A uniform contact between the particle and the crystal with minimal deformation was obtained applying sufficient pressure to the auto-level sapphire anvil [22]. Minimal deformation was ensured, such that the same particle could be picked up using the same needle without leaving any residue on the ATR crystal. After collecting a 'dry' image at 37 °C, ~2 ml of D_2O that had been pre-heated to 37 °C was injected into the cell in such a way that access to the particle was limited to the sides only as shown in Fig. 1. The raw images were collected in rapid scan mode taking ~5 min using the Agilent Technologies' ResolutionsPro FTIR Spectroscopy software version 5.2.0(CD846) with 128 co-added scans at an 8 cm^{-1} spectral resolution, and processed by ratioing against a background of the blank ATR crystal with 256 co-added scans also collected at 37 °C.

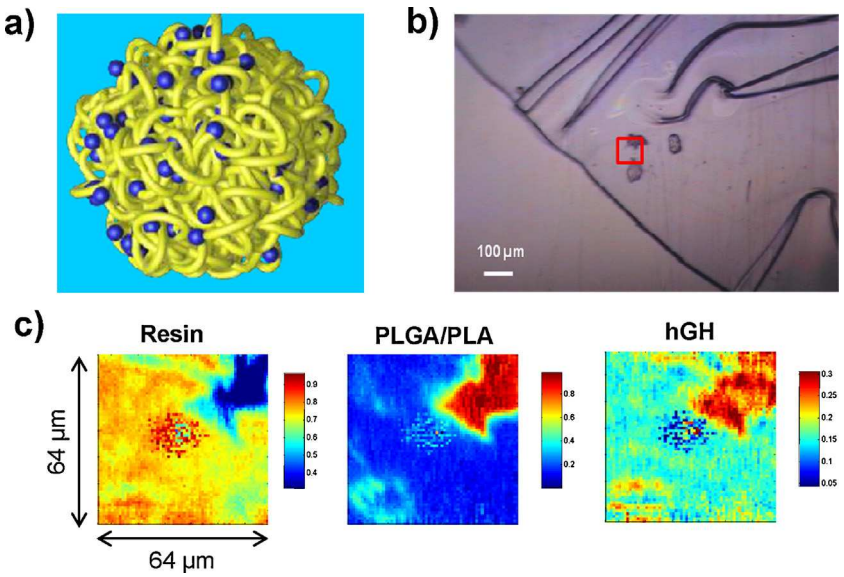

Fig. 2. (a) An illustration of a typical, CriticalMix™ processed microparticle where strands represent mixed polymers and dots represent the homogenously distributed hGH particles. (b) White light image of 3 microparticles embedded in resin and microtomed to 4 µm thickness (c) Micro ATR (Ge) peak height images from the area shown with the box in the white light image, showing resin (1724 cm^{-1}), PLGA/PLA (1755 cm^{-1}) and hGH (1650 cm^{-1}) from left to right respectively.

2.9. Data processing

Hyperspectral image cubes were processed using Malvern Instruments' ISys 5.0 chemical imaging software. Raw processed image files were cropped between 1820 and 1000 cm^{-1}, a region which contains a number of characteristic bands associated with PLGA/PLA polymers, protein amide I band ~1650 cm^{-1} and the δ(OD) band of D_2O at ~1207 cm^{-1}.

A Savitzky–Golay second derivative with a polynomial order of 3 and filter length of 29 was applied to cropped imaging data in order to eliminate baseline drift. Second derivative images were then vector normalised in order to remove systematic discrepancies such as variations in detector sensitivity or sample contact and therefore to minimise intensity (Log(1/R)) variance.

3. Results and discussion

ATR-FTIR spectroscopy facilitates the generation of chemical fingerprints of individual species and permits the monitoring of reaction and/or release kinetics due to the fact that unique molecular vibrations within a mixture can be assigned to different components within that mixture. As the evanescent wave effectively limits sample thickness, strongly absorbing molecules such as water can be observed facilely and this opens up the opportunity to observe systems where a sample is placed in contact with an aqueous medium. FTIR imaging permits the collection of temporal images of such multicomponent systems in aqueous media in which changes in the chemistry of such species can be spatially resolved in real time. In pharmaceutical research, this hyperspectral imaging approach using non-destructive IR light, particularly in ATR mode requiring no sample preparation or the use of dyes or chemical labels, is a unique toolbox for formulation design allowing characterisation of static samples, with as high as ~4 µm spatial resolution in micro mode, whilst facilitating the monitoring of dynamic physical and chemical changes occurring within formulations [10].

The CriticalMix process is thought to produce an homogenous distribution of API throughout the porous microparticles as

Table 1
Vibrational assignments for PLGA 50/50, PLA, Poloxamer 407, resin, D_2O and hGH within the finger print region (1820–1000 cm^{-1}); as antisymmetric, s symetric, δ bending, ρ rocking, ν stretching, τ twisting, ω wagging, all given in cm^{-1}.

PLGA	PLA	hGH	Poloxamer 407	Resin	D_2O	Assignment
1745	1745			1727		ν(C═O)
		1658				Amide I, ν(C═O)
				1635		δ(OH)
		1540				Amide II, δ(NH)
1452	1450	1450	1466	1484		$\delta_{as}(CH_3)$
1422				1450		δ(CH)
1394		1394		1395		ω(CH)
1381	1379		1374			$\delta_s(CH_3)$
1360	1362	1304	1359, 1341	1323		δ(CH)
1270	1266		1280, 1241	1274, 1249		$\tau(CH_2)$
		1245				ν_{as}(PO)
					1207	δ(OD)
1167	1184	1146	1144, 1100	1154		ν_{as}(COC)
1131	1127					$\rho_{as}(CH_3)$
		1104				ν_s(PO)
1086	1084	1077		1074		ν_s(COC)
1048	1045	1049	1059	1020		ν(C—CH_3)
		990				ν_s(PO)
957	957	942	962	948		$\rho(CH_3)$

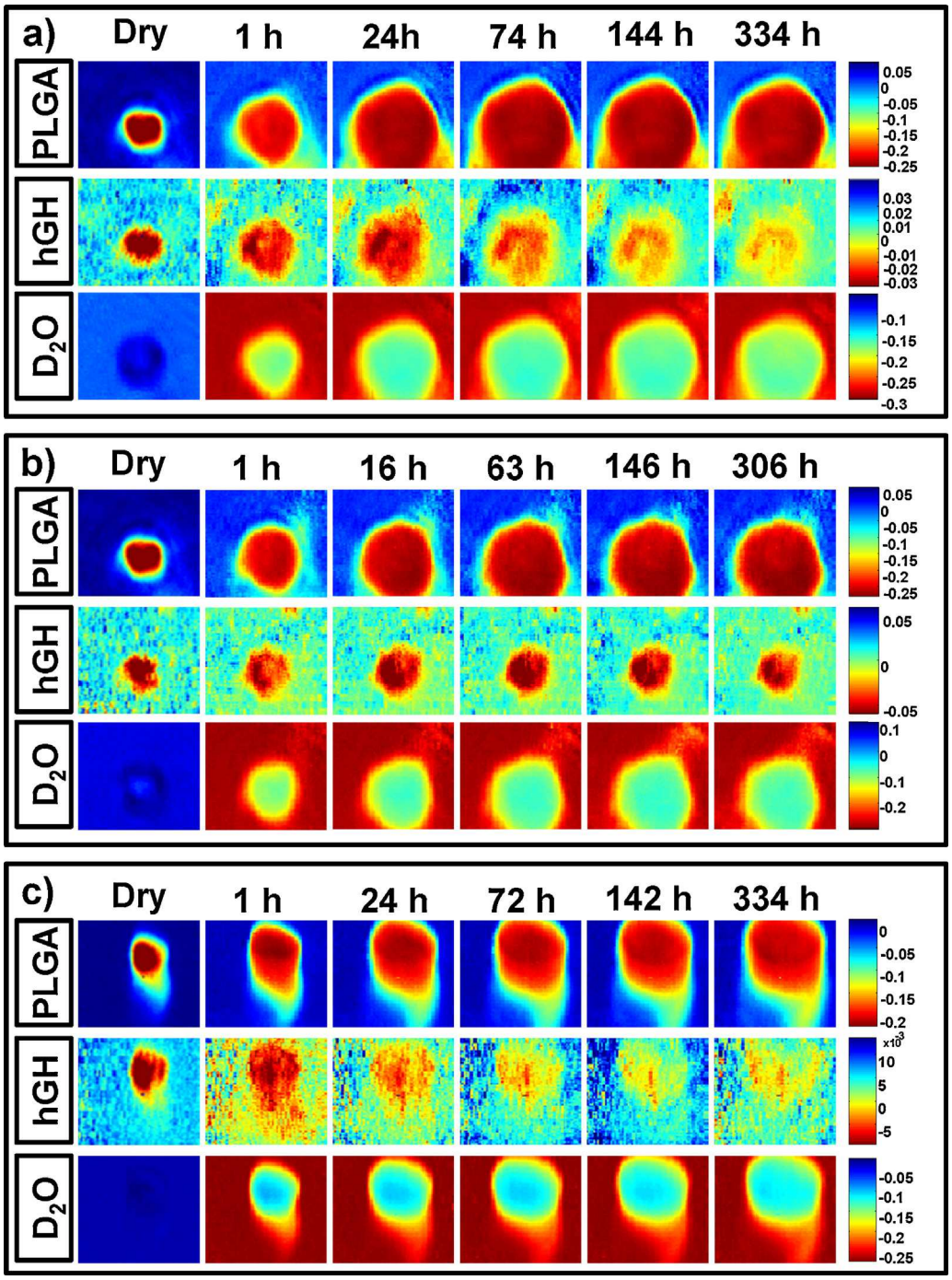

Fig. 3. False colour ATR-FTIR images of (a) non-irradiated, (b) 25 kGy γ-irradiated and (c) 100 kGy γ-irradiated microparticles showing second derivative peak height distribution of PLGA at 1755 cm^{-1}, hGH at 1650 cm^{-1} and D_2O at 1207 cm^{-1} as a function of time.

depicted in the illustration in Fig. 2(a). This was evaluated by microtoming a 4 μm section of a group of microparticles within an embedding medium highlighted by the red box in Fig. 2(b). Using mid-IR imaging in micro-ATR mode utilising a Ge ATR crystal which provided a spatial resolution of ~4 μm within ~64 μm × 64 μm field of view, the distribution of polymer and API within these particles was determined.

Table 1 shows the list of important peaks included in fingerprint region of the ATR-FTIR spectra obtained from pure samples. From this table, it can be seen that the most intense poloxamer 407 peaks overlap with PLGA/PLA peaks however very strong peaks are readily available at discrete wavenumbers for the rest of the samples. Also it will be discussed later on in the macro-ATR images, the δ(OD) of D_2O also becomes distinct when a second derivative is applied.

Fig. 2(c) shows the integrated peak height distribution of the resin at 1727 cm^{-1}, PLGA/PLA at 1755 cm^{-1} and hGH at 1650 cm^{-1} from left to right respectively. The distribution of PLGA/PLA and hGH, middle and right hand side images in Fig. 2(c) respectively, clearly show a good correlation between the high intensity (red) regions of PLGA/PLA and hGH. This is in contrast to the resin distribution, which shows an anti-correlation to both components. This is strong evidence of the homogenous distribution of hGH protein with in the PLGA/PLA microparticle layer.

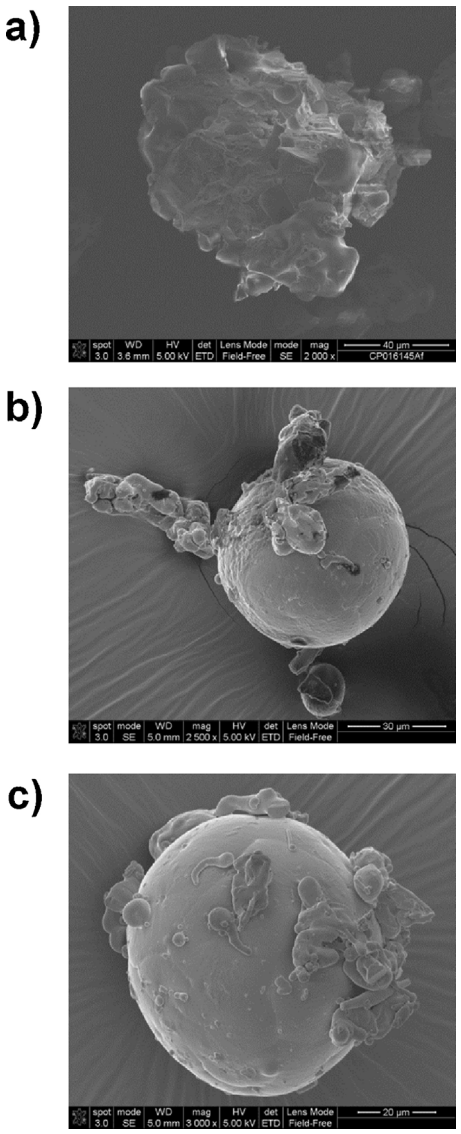

Fig. 4. SEM images showing typical (a) non-irradiated, (b) 25 kGy and (c) 100 kGy γ-irradiated microparticles.

FTIR imaging in macro-ATR mode has been demonstrated to facilitate imaging a variety of temporal information such as the morphological evaluation of different components, redistribution and/or release of species at polymer/solvent interfaces and the occurrence of new species during chemical reactions under the conditions of interest [10,12,15,23]. However release of active pharmaceutical ingredients (APIs) form single polymeric microparticles and monitoring the redistribution of API 'inside' a microparticle has not previously been studied by ATR-FTIR imaging.

To investigate the morphological and chemical evolution of a protein loaded polymeric microparticle in real time using ATR-FTIR imaging in macro mode and to explore the effect of γ-irradiation on such protein loaded PLGA/PLA microparticles, we have taken 3 single microparticles that had been subjected to γ-irradiation at doses of 25 and 100 kGy, as well as a control sample (same formulation without γ-irradiation) and monitored their interaction with water as a function of time at 37 °C. The experiment is setup in such a way that the interaction between the particle and water will only occur at the interfaces that we are monitoring, effectively creating a 2D experiment.

Fig. 3(a) shows six false colour images obtained by plotting the intensity distribution of the PLGA/PLA ester carbonyl (1755 cm^{-1}), protein (hGH) Amide I (1650 cm^{-1}) and D_2O δ(OD) (1207 cm^{-1}). The first column of images show the distribution of polymer, hGH and D_2O, respectively, before the dissolution experiment was started and are therefore labelled 'dry'. From these 'dry' images a homogenous distribution of hGH within the polymer matrix can be observed once again, complementing the micro-ATR image of the sliced sample shown in Fig. 2(c). Therefore we have confidence that the surface (up to ~10 μm) we are probing with IR light in this experiment is representative of internal structure of the microparticle, as expected from the CriticalMix™ manufacture of drug loaded microparticles [2,3].

The first row of images shown in Fig. 3(a) shows the change in the distribution of the PLGA/PLA component of the control, *i.e.* un-irradiated, hGH loaded PLGA/PLA microparticle. To a first approximation this set of images can be used to monitor the dimensional changes of the microparticle during the dissolution experiment. In the PLGA/PLA image collected after 1 h, image set there is evidence of an interface layer of hydrated PLGA/PLA around the particle even at this short time, with a decreasing D_2O concentration from the aqueous dissolution medium towards the particle centre and some evidence of particle swelling. Within 24 h the PLGA/PLA microparticle (red) appears to have swollen further, becoming larger, whilst still being surrounded by a hydrated PLGA/PLA layer (yellow), and over time the size of the particle stays almost the same in terms of visual representation. The bottom row of Fig. 3(a), shows the complementary image data set of D_2O distribution as a function of time. These images show a strong anti-correlation with the PLGA/PLA image dataset and verify the significant amount of swelling in this system, as one might expect, due to the inclusion of the excipient Poloxamer 407 at 9% (w/w) in the formulation, making the microparticles more hydrophilic [24,25]. It is worth noting that after ~1 h, D_2O is present, albeit at a low level, everywhere within the particle, almost certainly due to a combination of the particle hydrophilicity and its porosity. Over the duration of this experiment (334 h, ~14 days) we cannot observe any major evidence of 'shrinking' of the PLGA/PLA particle, implying this observation would require a much longer sampling period, perhaps several months at 37 °C. This not only shows the well-documented suitability of PLGA and PLA to act as biodegradable drug carriers, providing sustained release for several weeks to months, but also suggests that protein release from this system is dominated by diffusion rather than erosion, during the first 2 weeks, which may be expected due to the system being porous. The hGH distribution images (middle row, Fig. 3(a)), were generated by plotting the Amide I peak height at ~1650 cm^{-1}, show a change in the distribution at short times (<24 h) as the polymers are initially swollen and this is followed by a gradual decrease of overall hGH intensity distribution as a function of time. It is worth noting that the dimensions of the hGH rich region are somewhat smaller than their polymer and D_2O counterparts. One explanation for this is that the hGH is being lost into the D_2O media at the interfaces.

Fig. 3(b) shows the equivalent false colour infrared images for the data described in Fig. 3(a), obtained from a hGH loaded PLGA/PLA microparticle that has been subjected to 25 kGy γ-irradiation. The PLGA/PLA and D_2O distribution maps are quite similar to those shown in Fig. 3(a), and the hGH distribution images are once more much smaller than both the polymer and D_2O images. Any change to the colour intensity of the hGH rich region as a function of time after 24 h is more difficult to ascertain by visual inspection.

Fig. 3(c) shows analogous image data sets for a hGH loaded PLGA/PLA microparticle that has been subjected to 100 kGy γ-irradiation, and although at first glance the polymer and D_2O

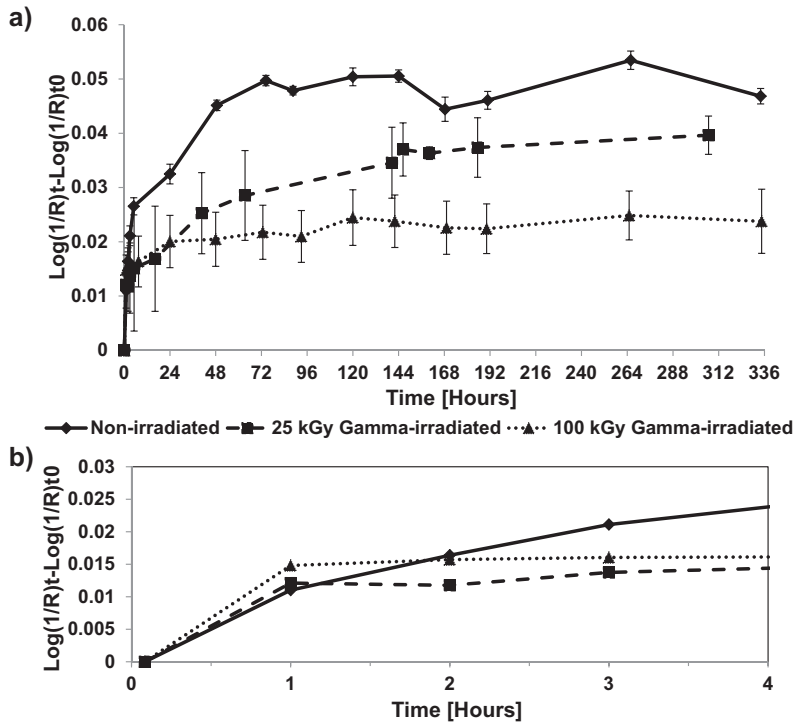

Fig. 5. (a)Release profiles obtained from 5 × 5 pixels regions of images of non-irradiated and γ-irradiated microparticles undergoing dissolution. Error bars indicate standard deviation between 3 ROIs used to obtain each data point.(b) The first 4 h data shown in (a), to provide clarity error bars are removed.

distribution images look similar to those depicted in Fig. 3(a) and (b), a remarkable rapid release of hGH around the microparticle can be seen in the 1 h image and to a lesser extent, in 24 h image, this may be due to the hGH being dissolved in the surrounding media during the ensuing 23 h. The subsequent time resolved hGH distribution maps contain fewer red pixels (*i.e.* high intensity regions) within the hGH images compared to the earlier time points, therefore it can be assumed that the most of hGH has been released during this initial hydration process; the so called burst release effect. Subsequent time resolved images show a slow reduction in intensity of the hGH distribution maps. Closer inspection of the D_2O distribution maps, show a higher concentration of D_2O (as denoted by the blue/green colour) within the body of the microparticle from 1 h when compared to both the un-irradiated and 25 kGy γ-irradiated hGH loaded microparticles.

It is clear that both geometry and morphology could have a strong influence on the release characteristics of a hGH loaded polymer microparticle, with porosity in particular likely to determine the rate of hydrolytic degradation and therefore drug release from such systems [26]. SEM was used to explore the morphology of the non-irradiated and irradiated microparticles. SEM is a tool that is readily applied to the microscopic characterisation of particles and other polymer surfaces [27].

Fig. 4 shows the SEM images of (a) non-irradiated, (b) 25 kGy γ-irradiated and (c) 100 kGy γ-irradiated microparticles. There are clear differences in morphology between the different microparticles, the γ-irradiated particles have a smooth surface and appear to be non-porous but with significant amounts of irregular particles, possibly hGH, attached to the surface. However the non-irradiated particle has a rough, non-uniform and porous morphology with inherently higher surface area than the γ-irradiated microparticles.

The use of FTIR imaging data to monitor drug release has been validated previously using an experimental setup that combined a UV detector to monitor the release of API from a tablet subjected to water flow during macro ATR-FTIR imaging and compared this to conventional dissolution test data of the same sample type [28]. Release profiles obtained from the two methods were shown to be very similar. By conducting measurements *in situ* using FTIR imaging, we can follow chemical changes by monitoring specific IR bands of components in a fixed area in a temporal image set and quantify the relative amount of that species released during a dissolution process. In each set of temporal images; non-irradiated, 25 kGy irradiated and 100 kGy irradiated, we have chosen 3 square regions (50 μm × 50 μm) of interest (ROI) from hGH rich zones within the microparticles by visually assessing the 1 h images in each data set. By calculating the decrease in area under amide-I peak at ~1650 cm^{-1} in the binned, normalised temporal spectra from the ROIs we can generate a release profile by assuming the decrease in hGH signal at time = *t* (compared to hGH signal at time = 0) is proportional to hGH released at that time point. Using this approach it is feasible to generate a dissolution plot that is analogous to a release profile from a standard USP I UV-dissolution experiment.

Fig. 5(a) shows the 3 release profiles obtained from temporal image sets of 0, 25 kGy and 100 kGy γ-irradiated hGH loaded microparticles shown in Fig. 3(a), (b) and (c), respectively, including additional time points for images not shown. Data points in Fig. 5(a) are generated from the average of overall intensity from the 3 binned and normalised ROIs and error bars indicate standard deviation. It is evident that in Fig. 5(a) for all three release profiles there are two distinct regions; firstly a rapidly increasing initial period followed by a second phase that almost represents a first order line profile with a slope close to zero.

In Fig. 5(b), this initial period in Fig. 5(a) up to 4 h, is plotted once again for better visualisation for evaluation of the burst release phenomenon. The release profile from the non-irradiated hGH loaded microparticle is showing an initial burst within the first few hours followed by a slower rate release for the duration of the experiment reaching a plateau sometime after ~72 h. This release profile, obtained from a single microparticle, is very similar to the release profile obtained by standard dissolution testing using UV detection [3] for the 10 mg of a similar formulation, both suggesting a

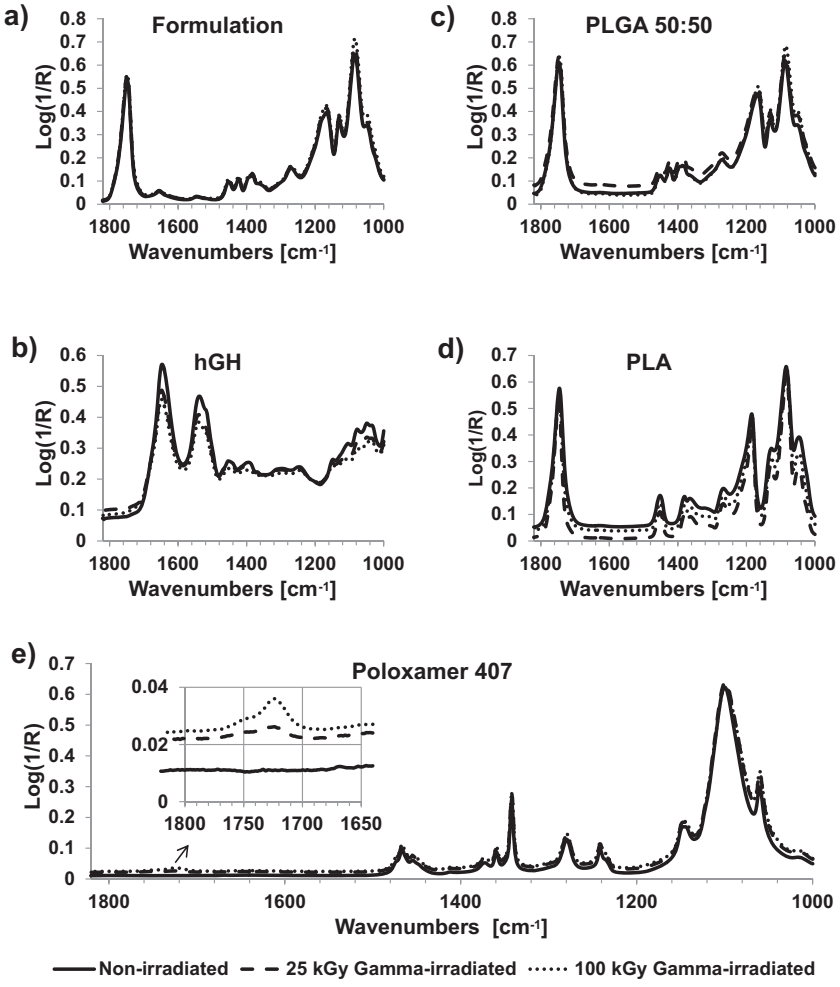

Fig. 6. ATR-FTIR spectra of non-irradiated and γ-irradiated; (a)formulation, (b)hGH, (c)PLGA50/50, (d)PLA and (e)Poloxamer 407.

rapid initial release based on diffusional escape through the pores existing in the microparticles, followed by a slower sustained release based on degradation of the polymers, indicating a high encapsulation efficiency (~100% [3]).

Fig. 5(a) also indicates that the total hGH release from the irradiated formulations is lower overall and particularly after reaching the plateau levels compared to the non-irradiated microparticle. This may be due to changes in the particle morphology, changes in the chemistry of the microparticle or some combination of the two.

The hGH release profile from the hGH loaded PLGA/PLA microparticle which has undergone 100 kGy irradiation, once again, shows a markedly high initial burst release particularly within the first 2 h (Fig. 5(b)) which was also evident in Fig. 3(c) in the 1 h image compared to the rest of the images in that row, indicating an immediate and high release of hGH that is too fast to be a polymer degradation or diffusion controlled. γ-irradiation causing this kind of an increased burst effect was also reported by Carrascosa et al. [29] who investigated recombinant human insulin-like growth factor-I (rhIGF-I) release from PLGA microspheres by SEM, UV-dissolution and differential scanning calorimetry (DSC). It is also evident from the SEM images that the 100 kGy irradiated hGH loaded microparticle has a smooth surface and appears have a non-porous morphology (Fig. 4(c)) compared to the very porous non-irradiated particle (Fig. 4(a)), therefore the initial burst from 100 kGy γ-irradiated particle is likely to be occurring due to surface bound hGH, that is made available at the surface of the microparticle during the γ-irradiation process. Unlike both the un-irradiated and the 25 kGy γ-irradiated sample, following its burst release, the 100 kGy γ-irradiated formulation shows zero measurable release after 48 h. For the non-irradiated and 25 kGy γ-irradiated microparticles it takes about up to 3 days for this to be the case. It is also worth remarking that the total amount of hGH that is being released after the initial burst appears to be much less than is observed in the other microparticles.

The release from the 25 kGy γ-irradiated formulation shows similarities to both the non-irradiated and the 100 kGy γ-irradiated microparticles; its initial burst profile is similar to the 100 kGy γ-irradiated formulation, indicating high protein availability at its surface, but it takes longer to reach a plateau similarly to that observed in the non-irradiated microparticle and the total amount of protein released appears to be in between that of non-irradiated and 100 kGy γ-irradiated samples, indicating an intermediate level of protein release due to degradation of the polymers at longer times. Considering the morphology of the 25 kGy γ-irradiated microparticles (Fig. 4(b)) being very similar to typical 100 kGy γ-irradiated particles; non-porous and smooth, a lower amount of release at longer times when compared to non-irradiated particles could be expected. This is a finding which is in agreement with that of Dorati et al. [5] who studied effect of γ-irradiation on PLGA microparticles containing ovalbumin using a combination of NMR, SEM and EPR.

Single point ATR-FTIR spectroscopy, collecting the average IR signal from a sample facilitates very high signal to noise ratio (S/N) in each spectrum when compared to imaging with an FPA

IR detector, hence may provide much more detailed vibrational information that may not be readily obtained from data collected using FPA detectors in imaging mode. Therefore in order to assess the effect of γ-irradiation on the chemistry of the microparticles and therefore infer their influence on hGH release, we also conducted ATR-FTIR measurements on bulk samples (both γ-irradiated and un-irradiated).

Fig. 6 shows the fingerprint region (1820–1000 cm^{-1}) of ATR-FTIR spectra of the non-irradiated, 25 kGy γ-irradiated and 100 kGy γ-irradiated hGH loaded micropartcles and pure components of the formulation. No noticeable change in the infrared spectra was observed as a result of being subjected to γ-irradiation on the hGH loaded microparticles, the PLGA, PLA or hGH components. (Fig. 6 (a)–(d)).

However, close inspection of the data collected from the Poloxamer 407 samples showed the appearance of a carbonyl band with increasing intensity proportional to the applied γ dose, indicating γ-irradiation induced degradation. Poloxamers are excipients that are used in drug carriers, such as PLGA micro or nano particle formulations, to enhance the release of drugs [24,25]. Therefore the degradation of Poloxamer407 is likely to have an impact on the release rate of the hGH loaded samples. When subjected to γ-irradiation, polymers may undergo chain scission or cross-linking. Dorati et al. [4] have shown that for PEG based polymers at higher γ-irradiation doses, chain scission is the predominant process leading to a greater number of oxygenated species and shorter PEG chain lengths. Increasing the number of oxygenated species in a microparticle is likely to have a significant impact on the dynamics of hydration due to an increase in the hydrophilicity and the strength and nature of interactions occurring between the species contained within that microparticle. In this instance, the increase in the number of oxygenated species appears to have significantly increased the rate of hydration, leading to a faster and more pronounced initial burst release of hGH. The increase in the number of oxygenated species within the microparticle may also influence the strength of interactions between the polymeric species and the encapsulated hGH, leading to a retardation of the sustained release rate after the initial burst. These findings are in agreement with those of Dorati et al. [5] who ascribed a retardation in the release rate of OVA from γ-irradiated PLGA-PEG microspheres, when compared to their un-irradiated counterparts, to be due to a combination of changes in the morphology of the microparticles and an increase in the magnitude of the interaction between the polymer matrix and the protein. Although our system is not identical to that studied by Dorati and co-workers [5], Poloxamer 407 is a tri-block copolymer of PEG-PPG-PEG, therefore we can anticipate the effect of γ-irradiation on these hGH loaded microparticles to be quite similar.

4. Conclusions

ATR-FTIR has been shown to be a successful method to monitor, *in situ*, the release of hGH from PLGA/PLA microparticles, providing important information about the mechanism of release. Utilising the chemical selectivity of the infrared methodology, hGH release profiles, analogous to those obtained using standard dissolution apparatus have been obtained for microparticles subjected to a range of γ-irradiation doses. The release mechanism of hGH from these microparticles has been elucidated with the release kinetics changing as a result of modifications to the microparticle morphology and chemistry during γ-irradiation. SEM analysis of the microparticles indicated that γ-irradiation made them less porous, reduced the surface area and forced some material, most likely hGH to the surface. FTIR-ATR analysis of the individual microparticle components, indicated that γ-irradiation was leading to chain scission in the Poloxamer 407 excipient, increasing the number of oxygenated species within the microparticle and influencing the strength of interactions between the entrapped hGH and the polymeric matrix. These findings are in good agreement with work conducted by Dorati et al. [5] and Carrascosa et al. [29] on PLGA based microparticles containing different protein based APIs.

Acknowledgement

The authors would like to thank the Engineering and Physical Sciences Research Council (EPSRC), grant number EP/I501665/1, for supporting this work.

References

[1] C. Wischke, S.P. Schwendeman, Int. J. Pharm. 364 (2008) 298–327.
[2] M.J. Whitaker, J. Hao, O.R. Davies, G. Serhatkulu, S. Stolnik-Trenkic, S.M. Howdle, K.M. Shakesheff, J. Control. Release 101 (2005) 85–92.
[3] F. Jordan, A. Naylor, C.A. Kelly, S.M. Howdle, A. Lewis, L. Illum, J. Control. Release 141 (2010) 153–160.
[4] R. Dorati, C. Colonna, M. Serra, I. Genta, T. Modena, F. Pavanetto, P. Perugini, B. Conti, AAPS PharmSciTech 9 (2008) 718–725.
[5] R. Dorati, I. Genta, L. Montanari, F. Cilurzo, A. Buttafava, A. Faucitano, B. Conti, J. Control. Release 107 (2005) 78–90.
[6] C. Martínez-Sancho, R. Herrero-Vanrell, S. Negro, J. Control. Release 99 (2004) 41–52.
[7] M.B. Sintzel, A. Merkli, C. Tabatabay, R.t. Gurny, Drug Dev. Ind. Pharm. 23 (1997) 857–878.
[8] T. Ribar, J.L. Koenig, R. Bhargava, Macromolecules 34 (2001) 8340–8346.
[9] C.A. Coutts-Lendon, N.A. Wright, E.V. Mieso, J.L. Koenig, J. Control. Release 93 (2003) 223–248.
[10] S.G. Kazarian, K.L.A. Chan, Macromolecules 36 (2003) 9866–9872.
[11] K.L.A. Chan, S.G. Kazarian, Vib. Spectrosc. 35 (2004) 45–49.
[12] R. Salzer, H.W. Siesler, Infrared and Raman Spectroscopic Imaging, Wiley-VCH, US, 2009.
[13] N.J. Everall, I.M. Priestnall, F. Clarke, L. Jayes, G. Poulter, D. Coombs, M.W. George, Appl. Spectrosc. 63 (2009) 313–320.
[14] S.E. Glassford, L. Govada, N.E. Chayen, B. Byrne, S.G. Kazarian, Vib. Spectrosc. 63 (2012) 492–498.
[15] K.L.A. Chan, S.G. Kazarian, Appl. Spectrosc. 64 (2010) 135A–152A.
[16] J.F. Carpenter, J.H. Crowe, Biochemistry 28 (1989) 3916–3922.
[17] T. Yang, A. Dong, J. Meyer, O.L. Johnson, J.L. Cleland, J.F. Carpenter, J. Pharm. Sci. 88 (1999) 161–165.
[18] K. Fu, K. Griebenow, L. Hsieh, A.M. Klibanov, Robert Langera, J. Control. Release 58 (1999) 357–366.
[19] M. van de Weert, R. van't Hof, J. van der Weerd, R.M.A. Heeren, G. Posthuma, W.E. Hennink, D.J.A. Crommelin, J. Control. Release 68 (2000) 31–40.
[20] S.G. Kazarian, K.W.T. Kong, M. Bajomo, J. Van Der Weerd, K.L.A. Chan, Food Bioprod. Process. 83 (2005) 127–135.
[21] P.S. Wray, G.S. Clarke, S.G. Kazarian, Eur. J. Pharm. Sci. 48 (2013) 748–757.
[22] G. Thomson, G. Poulter, US Patent US20060261274 A1 (2006).
[23] J. van der Weerd, K.L.A. Chan, S.G. Kazarian, Vib. Spectrosc. 35 (2004) 9–13.
[24] F. Yan, C. Zhang, Y. Zheng, L. Mei, L. Tang, C. Song, H. Sun, L. Huang, Nanomed. Nanotechnol. Biol. Med. 6 (2010) 170–178.
[25] G. Dumortier, J.L. Grossiord, F. Agnely, J.C. Chaumeil, Pharm. Res. 23 (2006) 2709–2728.
[26] H.K. Kim, T.G. Park, J. Control. Release 98 (2004) 115–125.
[27] V. Klang, C. Valenta, N.B. Matsko, Micron 44 (2013) 45–74.
[28] J. van der Weerd, S.G. Kazarian, J. Control. Release 98 (2004) 295–305.
[29] C. Carrascosa, L. Espejo, S. Torrado, J.J. Torrado, J. Biomater. Appl. 18 (2003) 95–108.